

Spatially explicit predictions of food web structure from regional level data

Tracked changes version

Gabriel Dansereau

Ceres Barros

Timothee Poisot

Abstract

Knowledge about how ecological networks vary across global scales is currently limited given the complexity of acquiring repeated spatial data for species interactions. Yet, recent developments of metawebs highlight efficient ways to first document possible interactions within regional species pools. Downscaling metawebs towards local network predictions is a promising approach to use current data to investigate the variation of networks across space. However, issues remain in how to represent the spatial variability and uncertainty of species interactions, especially for ~~large-scale~~ large-scale food webs. Here, we present a probabilistic framework to downscale a metaweb based on the Canadian mammal metaweb and species occurrences from ~~GBIF. We investigate~~ global databases. We investigated how our approach can be used to represent the variability of networks and communities between ecoregions in Canada. ~~Our results highlighted mismatches in the distribution of species~~ Species richness and interactions ; ~~especially in their within-ecoregion variability, indicating that interactions vary differently than species distributions over continental-scale gradients. Results summarized by ecoregion showed non-constant variation within and between ecologically meaningful biogeographic boundaries and~~ followed a similar latitudinal gradient across ecoregions but at the same time identified contrasting diversity hotspots. Network motifs revealed additional areas of variation in network structure compared to species richness

[and number of links](#). Our method offers the potential to bring global predictions down to a more actionable local scale, and increases the diversity of ecological networks that can be projected in space.

Introduction

Because species interactions vary in time and space, and because species show high turnover over larger spatial extents, adequately capturing the diversity of ecological networks is a challenging task (Jordano 2016). Most studies on food webs have previously focused on local networks limited in size and extent, and are rarely replicated in space or time (Mestre *et al.* 2022). Interactions can show important variations in space (Poisot *et al.* 2015; Zarnetske *et al.* 2017), yet available network data also show important geographical bias by focusing sampling efforts in a few areas or biomes, limiting our ability to answer questions in many biomes and over broad spatial extents (Poisot *et al.* 2021). Moreover, global monitoring of biotic interactions is insufficient to properly describe and understand how ecosystems are reacting to global change (Windsor *et al.* 2023). Approaches to predict species interactions (e.g., Morales-Castilla *et al.* 2015; Desjardins-Proulx *et al.* 2017) are increasingly used as an alternative to determine potential interactions; they can handle limited data to circumvent data scarcity (Strydom *et al.* 2021), but are still rarely used to make explicitly spatial predictions. As a result, there have been repeated calls for globally distributed interaction and network data coupled to repeated sampling in time and space (Mestre *et al.* 2022; Windsor *et al.* 2023), which will help understand the macroecological variations of food webs (Baiser *et al.* 2019).

Despite these limitations, food web ecologists often can infer a reasonable approximation of the network existing within a region. This representation, called a metaweb, contains all possible interactions between species in a given regional species pool (Dunne 2006), and provides a solid foundation to develop approaches to estimate the structure of networks at finer spatial scales.

43 When assembled by integrating different data sources (and potentially with additional predictive steps),
44 the metaweb allows to overcome sampling limitations and to raise network data to a global scale. For
45 example, Albouy *et al.* (2019) coupled data on fish distributions with a statistical model of trophic
46 interactions to provide estimates of the potential food web structure at the global scale. Recent studies
47 have focused on assembling metawebs for various taxa through literature surveys and expert elicitation
48 (European terrestrial tetrapods, Maiorano *et al.* 2020) or using predictive tools (marine fishes, Albouy
49 *et al.* 2019; Canadian mammals, Strydom *et al.* 2022). At a finer spatial scale, the local food webs
50 (i.e. the local “realization” of the metaweb when combined with species distributions, Poisot *et al.* 2012)
51 reflect local environmental conditions but still retain the signal of the metaweb to which they belong
52 (Saravia *et al.* 2022). Given this, Strydom *et al.* (2023) defended that predicting the metaweb’s structure
53 should be the core goal of predictive network ecology, ~~as if~~. Assuming there is a strong link between
54 the metaweb and its local realizations, more ~~accurate~~ accurate predictions of the metaweb will have
55 the potential to bring us closer to producing accurate local (downscaled) predictions (Strydom *et al.*
56 2023). Therefore, establishing or predicting the metaweb should be the first target in systems lacking
57 information about local realizations. This is not the same as using interactions to improve predictions
58 of species distributions, as recent studies have done (Moens *et al.* 2022; Poggiato *et al.* 2022; Lucas *et*
59 *al.* 2023), although these are incredibly relevant and answer long-standing calls to include interactions
60 within such models (Wisz *et al.* 2013). Instead, predicting networks in space is a different task, and it
61 serves a different goal: focusing first on the distribution of network structures and its drivers rather than
62 on the distribution of species.

63 Explicit spatial predictions (such as downscaled metaweb predictions) are essential as they will allow
64 comparisons with extant work for species-rich communities. Recent approaches to metaweb downscaling
65 combined a regional metaweb with species distribution maps to generate local assemblages for European
66 tetrapods (Braga *et al.* 2019; O’Connor *et al.* 2020; Galiana *et al.* 2021; Gaüzère *et al.* 2022), Barents

Sea marine taxa (Kortsch *et al.* 2019), and North Sea demersal fishes and benthic epifauna (Frelat *et al.* 2022). These downscaled assemblages allowed studying network structures in novel ways, for instance, assessing changes in food web structure across space (Braga *et al.* 2019), describing the scaling of network area relationships (Galiana *et al.* 2021). Other examples have shown that the metaweb can be used to investigate large-scale variation in food web structure, indicating high geographical connections and heterogeneous robustness against species extinctions (Albouy *et al.* 2019), which are only apparent when the local and global networks are both available. Further comparisons between network structure and other community properties are relevant as they may highlight new and surprising elements regarding network biogeography. For instance, Frelat *et al.* (2022) found a strong spatial coupling between community composition and food web structure, but a temporal mismatch depending on the spatial scale. Poisot *et al.* (2017) found that interaction uniqueness captures more composition variability than community uniqueness, and that sites with exceptional compositions might differ for networks and communities, because species distributions and species interactions had different bioclimatic drivers. Spatialized network data will allow these comparisons, identifying important conservation targets for networks and whether they differ geographically from areas currently prioritized for biodiversity conservation.

A key challenge remains in how to downscale a regional metaweb towards local network predictions that reflect the spatial variability of interactions. Even when the metaweb is known, local networks may vary substantially and differ both amongst themselves and from the metaweb (McLeod *et al.* 2021), emphasizing the need for methods to generate local, downscaled network predictions. A potential limitation to previous downscaling approaches is that they assume interactions are constant across space, which ignores well-documented interaction variability, and masks the effect of environmental conditions on interaction realization (Braga *et al.* 2019). In contrast, recent studies argued that seeing interactions as probabilistic (rather than binary) events allows us to account for their variability in space

(Poisot *et al.* 2016) and that this should also be reflected at the metaweb level (Strydom *et al.* 2023). Gravel *et al.* (2019) introduced a probabilistic framework describing how the metaweb can generate local realizations and showed how it could be used for modelling interaction distributions. This approach to downscaling is relevant when combined with *in situ* observations of interactions and local networks to train interaction models (in this case, with willow-galler-parasitoid networks). However, such data is rarely available across broad spatial extents (Hortal *et al.* 2015; Poisot *et al.* 2021; Windsor *et al.* 2023). Spatially replicated interaction data required for such models are especially challenging to document with large food web systems such as European tetrapod and Canadian mammal metawebs (Maiorano *et al.* 2020; Strydom *et al.* 2022), where hundreds of species result in tens of thousands of species pairs that may potentially interact. We currently lack a downscaling framework that is both probabilistic and can be trained without replicated *in situ* interaction data. Additionally, a probabilistic view can allow propagating uncertainty, which can play a key role in evaluating the quality of the predictions. Assessing model uncertainty would enable us to determine to which degree we should trust our predictions and to identify what to do to improve the current knowledge.

Here, we present a workflow to downscale a metaweb in space, and illustrate it by spatially reconstructing local instances of a probabilistic metaweb of Canadian mammals. We do so using a probabilistic approach to both species distributions and interactions in a system without spatially replicated interaction data. We then explore how the spatial structure of the downscaled metaweb varies in space and how the uncertainty of interactions can be made spatially explicit. We further show that the downscaled metaweb can highlight important biodiversity areas and bring novel ecological insight compared to traditional community measures like species richness.

Methods

Fig. 1 shows a conceptual overview of the methodological workflow leading to the downscaled metaweb. Its components were grouped as non-spatial and spatial data, localized site steps (divided into single-species-level, two-species-level, and network-level steps), and the final downscaled and spatialized metaweb. Throughout these steps, we highlight the importance of presenting the uncertainty of interactions and their distribution in space. We argue that this requires adopting a probabilistic view and incorporating variation between scales.

Data

Metaweb

The main source of interaction data was the metaweb for Canadian mammals from Strydom *et al.* (2022), which is a-spatial, i.e., it represents interactions between mammals that can occur anywhere in Canada. It contains 163 species and 3280 links with a probability of interaction. The species list for the Canadian metaweb was extracted from the International Union for the Conservation of Nature (IUCN) checklist (Strydom *et al.* 2022). Briefly, the metaweb was developed using graph embedding and phylogenetic transfer learning based on the metaweb of European terrestrial mammals, which is itself based on a comprehensive survey of interactions reported in the scientific literature (Maiorano *et al.* 2020). The Canadian metaweb showed a 91% success rate for known interactions between Canadian mammals recorded in global databases (Strydom *et al.* 2022). This metaweb is probabilistic, which has the advantage of reflecting the likelihood of an interaction taking place given the phylogenetic and trait match between two species. This allows incorporating interaction variability between species (i.e., taking into account that two species may not always interact whenever or wherever they occur); however, we highlight that other factors beyond trait and phylogenetic matching (e.g., population densities) will also

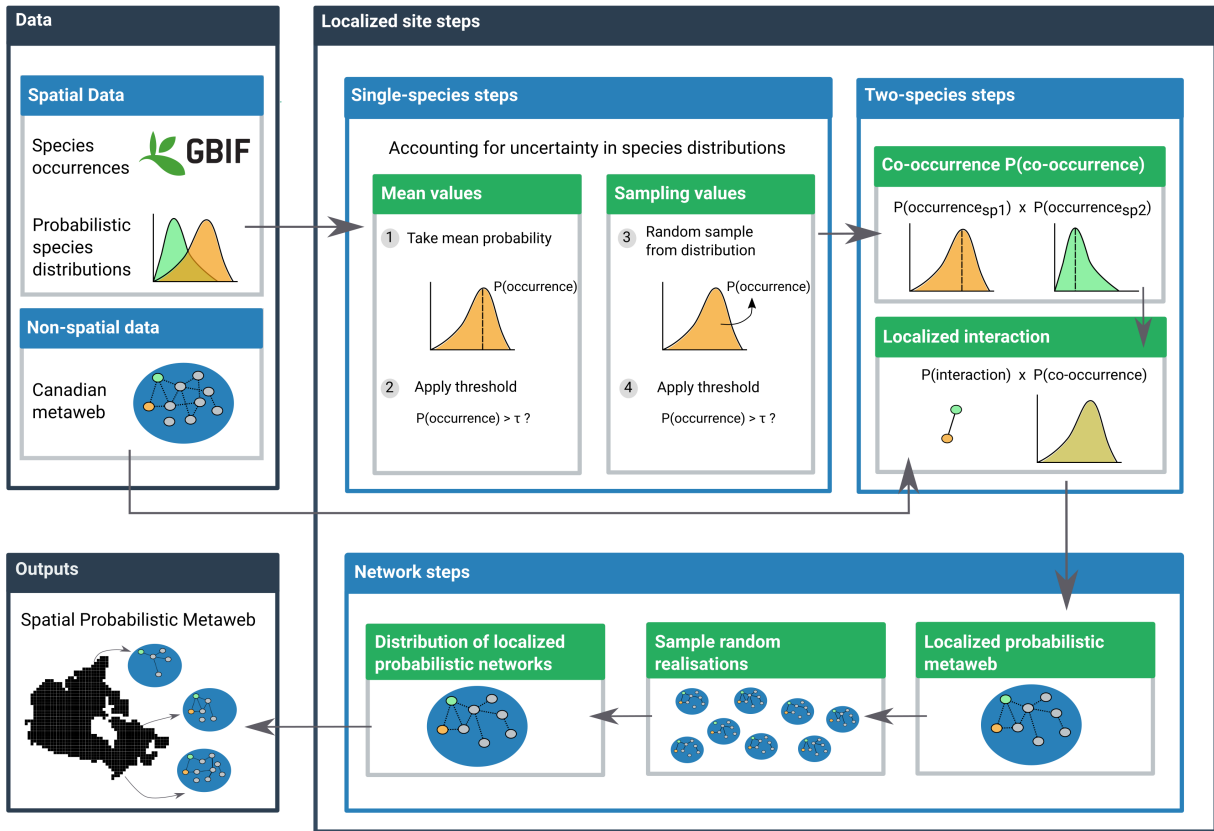


Figure 1: Conceptual figure of the proposed workflow used to downscale the probabilistic metaweb in space. The workflow has three components: the data, the localized steps, and the final spatial output. The data are composed of spatial data (with information in every cell) and non-spatial data (constant for all of Canada). The localized steps use these data and are performed separately in every cell, first at a single-species level (using distribution data), then for every species pair (adding interaction data from the metaweb), and finally at the network level by combining the results of all species pairs. The final output of the network-level steps contains a downsampled probabilistic metaweb for every cell across the study extent.

contribute to observed interaction frequencies.

Species occurrences

The downscaling of the metaweb involved combining it with species occurrence and environmental data. First, we extracted species occurrences from the Global Biodiversity Information Facility (GBIF; www.gbif.org) for the Canadian mammals after reconciling species names between the Canadian metaweb and GBIF using the GBIF Backbone Taxonomy (GBIF Secretariat 2021). This step removed potential duplicates by combining species listed in the Canadian metaweb which were considered as a single entity by GBIF. We collected occurrences for the updated species list (159 species) using the GBIF download API on October 21st 2022 (GBIF.org 2022). We restricted our query to occurrences with coordinates between longitudes 175°W to 45°W and latitudes 10°N to 90°N. This was meant to collect training data covering a broader range than our prediction target (Canada only) and include observations in similar environments. Then, since GBIF observations represent presence-only data and most predictive models require absence data, we generated the same number of pseudo-absence data ~~using the surface range envelope method, which selects random non-observed sites within the spatial range delimited by the presence data~~ (as occurrences for every species (Barbet-Massin *et al.* 2012). We weighted candidate sites by their distance to a known observation (separately for each species) using the DistanceToEvent method from the Julia package SpeciesDistributionToolkit (<https://github.com/PoisotLab/SpeciesDistributionToolkit.jl>), making it more likely to select sites further away from an observation and the known species range. This is because our intent was to model the potential distribution of species, capturing wider responses to the environment, as the downscaled metaweb we aimed to produce is potential in nature (see *Downscaled metaweb* section below).

Environmental data

We used species distribution models (SDMs, Guisan & Thuiller 2005) to project Canadian mammal habitat suitability across the country, which we treated as information on potential distribution. For each species, we related occurrences and pseudo-absences with 19 bioclimatic variables from CHELSA (Karger *et al.* 2017) and 12 consensus land-cover variables from EarthEnv (Tuanmu & Jetz 2014). The CHELSA bioclimatic variables (*bio1-bio19*) represent various measures of temperature and precipitation (e.g., annual averages, monthly maximum or minimum, seasonality) and are available for land areas across the globe. We used the most recent version, the CHELSA v2.1 dataset (Karger *et al.* 2021), and subsetting it to land surfaces only using the CHELSA v1.2 (Karger *et al.* 2018), which does not cover open water. The EarthEnv land-cover variables represent classes such as Evergreen broadleaf trees, Cultivated and managed vegetation, Urban/Built-up, and Open Water. Values range between 0 and 100 and represent the consensus prevalence of each class in percentage within a pixel (hereafter called sites). We coarsened both the CHELSA and EarthEnv data from their original 30 arc-second resolution to a 2.5 arc-minute one (around 4.5 km at the Equator) using GDAL (GDAL/OGR contributors 2021). This resolution compromised capturing both local variations and broad-scale patterns while limiting computation costs to a manageable level as memory requirements rapidly increase with spatial resolution.

Analyses

Species distribution models

Our selection criteria for choosing an SDM algorithm was to have a method that generated probabilistic results (similar to Gravel *et al.* 2019), including both a probability of occurrence for a species in a specific site and the uncertainty associated with the prediction. These were crucial to obtaining a probabilistic version of the metaweb as they were used to create spatial variations in the localized

interaction probabilities (see next section). One suitable method for this is Gradient Boosted Trees with a Gaussian maximum likelihood from the `EvoTrees.jl` *Julia* package (<https://github.com/EvoTrees/EvoTrees.jl>). This method returns a prediction for every site with an average value and a standard deviation, which we ~~used~~ considered as a measure of uncertainty. We used the average value and standard deviation to build a Normal distribution for the probability of occurrence of a given species at ~~all sites~~ each site (represented as probability distributions on Fig. 1). We trained models across the extent chosen for occurrences (longitudes 175°W to 45°W and latitudes 10°N to 90°N), then predicted species distributions only for Canada. We used the 2021 Census Boundary Files from Statistics Canada (Statistics Canada 2022) to set the boundaries for our predictions, which gave us 970,698 sites in total. Performance evaluation for the single species SDMs are available on GitHub.

Building site-level instances of the metaweb

The next part of the workflow was to produce local metawebs for every site (*Localized steps* box on Fig. 1). This component was divided into single-species, two-species, and network-level steps.

The single-species steps represented four possible ways to account for uncertainty in the species distributions and bring variation to the spatial metaweb. We explored four different options to select a value ($P(\text{occurrence})$; Fig. 1) from the occurrence distributions obtained in the previous steps: 1) taking the mean from the distribution as the probability of occurrence (option 1 in Fig. 1); 2) converting the mean value to a binary one using a specific threshold per species (option 2); 3) sampling a random value within the Normal distribution (option 3); or 4) converting a random value into a binary result (option 4, using a separate draw from option 3 and the same threshold as in option 2). The threshold (τ in Fig. 1) used was the value that maximized Youden's J informedness statistic (Youden 1950), the same metric used by Strydom *et al.* (2022) at an intermediate step while building the metaweb. The four sampling options were intended to explore how uncertainty and variation in the species distributions can affect

the metaweb result. We expected thresholding to have a more pronounced effect on network structure as it should reduce the number of links by removing many of the rare interactions (Poisot *et al.* 2016). On the other hand, we expected random sampling to create higher spatial heterogeneity compared to the mean probabilities, as including some extreme values should confound the ~~potential effects of~~ main trends promoted by environmental gradients. We chose option 1 to present our results as it is intuitive and essentially represents the result of a probabilistic SDM (as in Gravel *et al.* 2019), but results obtained with other sampling strategies are available in Supplementary Material, ~~Fig. S1~~.

Next, the two-species steps were aimed at assigning a probability of observing an interaction between two species in a given site. For each species pair, we multiplied the product of the two species' occurrence probabilities ($P(\text{co-occurrence})$; Fig. 1) (obtained using one of the sampling options above) by their interaction probability in the Canadian metaweb. For cases where species in the Canadian metaweb were considered as the same species by the GBIF Backbone Taxonomy (the reconciliation step mentioned earlier), we used the highest interaction probabilities involving the duplicated species.

The network-level steps then created the probabilistic metaweb for the site. We assembled all the local interaction probabilities (from the two-species steps) into a probabilistic network (Poisot *et al.* 2016). We then sampled several random network realizations to represent the potential local realization process (Poisot *et al.* 2015). This resulted in a distribution of localized networks, which we averaged over the number of simulations to obtain a single probabilistic network for the site.

Downscaled metaweb

The final output of our workflow was the downscaled metaweb, which contains a localized probabilistic metaweb in every site across the study area (*Outputs* box in Fig. 1). The metaweb sets an upper bound on the potential interactions (Strydom *et al.* 2023), therefore, the downscaled metaweb is a refined upper boundary at the local scale that takes into account co-occurrences. It is still potential in nature and

differs from a local realization, from which it should have a different structure. Nonetheless, from the downscaled metaweb, we can create maps of network properties (e.g. number of links, connectance) measured on the local probabilities of species interactions and occurrences, and compute some traditional community-level measures such as species richness. We chose to compute and display the expected number of links (measured on probabilistic networks following Poisot *et al.* 2016; see Gravel *et al.* 2019 for a similar example) as its relationship with species richness has been highlighted in a spatial context in recent studies (Galiana *et al.* 2021, 2022). We also computed the uncertainty associated with the community and network measurements (richness variance and link variance, respectively) and compared their spatial distribution (see Supplementary Material).

Analyses of results by ecoregions

Since both species composition and network summary values display a high spatial variation and complex patterns, we simplified the representation of their distribution by grouping sites by ecoregion, as species and interaction composition have been shown to differ between ecoregions across large spatial scales (Martins *et al.* 2022). To do so, we rasterized the Canadian subset of the global map of ecoregions from (Dinerstein *et al.* 2017; also used by Martins *et al.* 2022), which resulted in 44 different ecoregions. For every measure we report (e.g. species richness, number of links), we calculated the median site value for each ecoregion, as a way to avoid bias due to long tails in the distributions. We also measured within-ecoregion variation as the 89% interquantile range of the site values in each ecoregion (threshold chosen to avoid confusion with conventional significance tests; McElreath 2020).

Analyses of ecological uniqueness

We compared the compositional uniqueness of the networks and the communities to assess whether they indicated areas of exceptional composition. We measured uniqueness using the local contributions

to beta diversity (LCBD, Legendre & De Cáceres 2013), which identify sites with exceptional composition
 by quantifying how much one site contributes to the total variance in the community composition.
 While many studies used LCBD values to evaluate uniqueness on local scales or few study sites (for
 example, da Silva & Hernández 2014; Heino & Grönroos 2017), recent studies used the measure on
 predicted species compositions over broad spatial extents and a large number of sites (Vasconcelos *et al.* 2018; Dansereau *et al.* 2022). LCBD values can also be used to measure uniqueness for networks by
 computing the values over the adjacency matrix, which has been shown to capture more unique sites
 and uniqueness variability than through species composition (Poisot *et al.* 2017). Here, we measured and
 compared the uniqueness of our localized community and network predictions. For species composition,
 we assembled a site-by-species community matrix (970,698 sites by 159 species) with the probability of
 occurrence of each species at every site ~~from~~ obtained in the species distribution models. For network
 composition, we assembled a site-by-interaction matrix with the localized ~~interaction values from the~~
~~spatial probabilistic metaweb~~ probability of interaction at every site given by the downscaled metaweb
(therefore 970,698 sites by 3,108 interactions with defined probabilities in the metaweb). We applied
 the Hellinger transformation on both matrices and computed the LCBD values from the total variance
 in the matrices (Legendre & De Cáceres 2013). High LCBD values indicate a high contribution to the
 overall variance and a unique species or interaction composition compared to other sites. Since the
 values themselves are very low given our high number of sites (as in Dansereau *et al.* 2022), what
 matters primarily is the magnitude of the difference between the sites. Given this, we divided values
 by the maximum value in each matrix (species or network) and suggest that these should be viewed as
 relative contributions compared to the highest observed contribution. As with other measures, we then
 summarized the local uniqueness values by ecoregion by taking the median LCBD value and measuring
 the 89% interquantile range.

Analyses of network motifs

To further explore network structure in space, we investigated the distribution of network motifs across space. Motifs are defined sets of interaction between species (Milo *et al.* 2002; Stouffer *et al.* 2007), for instance two predators sharing one prey, which are repeated within larger and more complex food webs. Motifs are linked to community persistence (Stouffer & Bascompte 2010) and community structure (Cirtwill & Stouffer 2015; Simmons *et al.* 2019), are conserved across scales (Baker *et al.* 2015; Baiser *et al.* 2016), and are part of a common backbone of interactions among all food webs (Mora *et al.* 2018). We focused on four of the most studied three-species motifs (Stouffer *et al.* 2007; Stouffer & Bascompte 2010; Baiser *et al.* 2016) : S1 (tri-trophic food chains), S2 (omnivory), S4 (exploitative competition) and S5 (apparent competition). These motifs can be grouped into two pairs according to the ecological information they display: S1 and S2 highlight different trophic structures, while S4 and S5 identicate different competition types. Therefore, we compared the spatial distribution of the motifs in each pair to see which ones were dominant across all our sites. First, we computed the expected motif count for each of the four motifs for all sites using the localized probabilistic networks from the downscaled metaweb (following Poisot *et al.* 2016). Then, we compared the expected counts of the motifs within the two pairs. To do so, we used a measure of normalized difference similar to the Normalized Difference Vegetation Index (NDVI), where we compute the difference between the two motif counts over their sum. We called the index comparing the two trophic motifs (S1 and S2) the Normalized Difference Trophic Index (NDTI), and the one comparing the competition motifs (S4 and S5) the Normalized Difference Competition Index. We defined both indexes as:

$$NDTI = \frac{(S1 - S2)}{(S1 + S2)}$$

$$NDCI = \frac{(S4 - S5)}{(S4 + S5)}$$

Values for both indexes are bounded between -1 and 1. A value of 0 indicates that both motifs have the same expected counts. Positive values indicate that the first motif in each index (S1 and S4) is dominant and has a higher expected count, while negative values indicate that the second motif (S2 and S5) is dominant. As with previous measures, we then summarized both index values by ecoregion by taking the ecoregion median and measuring its within-ecoregion variation with the 89% interquartile range. Ecoregion values therefore indicate if one type of trophic structure (for NDTI) and one type of competition (for NDCI) is dominant in the ecoregion, while the interquartile range values measures whether the dominant type varies within the ecoregion.

We used *Julia* v1.9.0 (Bezanson *et al.* 2017) to implement all our analyses. We used packages GBIF.jl (Dansereau & Poisot 2021) to reconcile species names using the GBIF Backbone Taxonomy, SpeciesDistributionToolkit.jl (<https://github.com/PoisotLab/SpeciesDistributionToolkit.jl>) to handle raster layers, species occurrences and generate ~~pseudoabsences~~ pseudo-absences (using the [DistanceToEvent method](#)), EvoTrees.jl (<https://github.com/Evoest/EvoTrees.jl>) to perform the Gradient Boosted Trees, EcologicalNetworks.jl (Poisot *et al.* 2019) to analyze network and metaweb structure, and Makie.jl (Danisch & Krumbiegel 2021) to produce figures. Our data sources (CHELSA, EarthEnv, Ecoregions) were all unprojected, and we did not use a projection in our analyses. However, we displayed the results using a Lambert conformal conic projection more appropriate for Canada using GeoMakie.jl (<https://github.com/MakieOrg/GeoMakie.jl>). All the code used to implement our analyses is archived on Zenodo (<https://doi.org/10.5281/zenodo.8350065>; Dansereau & Poisot 2023) and includes instructions on how to run a smaller example at a coarser resolution. Note that running our analyses at full scale is resource and memory-intensive and required the use of computer clusters provided by Calcul Québec and the Digital Research Alliance of Canada. Full-scale computations

(excluding motifs) required 900 CPU core-hours and peaked at 500 GB of RAM. Computations for network motifs were even more intensive and required 12 CPU core-years.

Results

Our workflow allowed us to display the spatial distribution of ecoregion-level community measures (here, expected species richness) and network measures (expected number of links; Fig. 2). We highlight that the ~~community and network-level~~ measures presented here are ~~not actual predictions~~ first computed over the predicted communities and networks obtained when downscaling the metaweb, then summarized across the ecoregions (taking the median within each ecoregion). They are not a direct prediction of the measure itself (e.g., we do not present a prediction of actual species richness at each location). ~~Instead, they are the reflection of these metrics from the localized predictions of the communities and networks obtained from the downscaling of the metaweb, then summarized for the ecoregions (using the median value).~~—Expected ecoregion richness (Fig. 2A) and expected number of links (Fig. 2B) displayed similar distributions with a latitudinal gradient and higher values in the south. ~~However, within-ecoregion~~ Within-ecoregion variability was distributed ~~differently, as some ecoregions along the coast displayed higher interquantile ranges, while ecoregions around~~ slightly differently with a less constant latitudinal gradient, notably lower interquantile ranges near the southern border ~~displayed narrower ones ((for example, near Vancouver Island and the Rockies on the West Coast, and near the Ontario Peninsula, the Saint-Lawrence Valley, and Central New-Brunswick in the East; Fig. 2C-D).~~ Bivariate comparison of the distributions of species richness and expected number of links and of their respective within-ecoregion variability further shows some areas of mismatches, indicating that richness and links do not co-vary completely although they may show similar distributions for median values (see Supplementary Material, Fig. S1). All results shown are based on the first sampling strategy (option 1) mentioned in the *Building site-level instances of the metaweb* section, where we used the mean

value of the species distributions as the species occurrence probabilities (results for other sampling strategies are shown in Supplementary Material, Fig. [S1-S2](#)). Site-level results (before summarizing by ecoregion) are also provided in Supplementary Material (Figs. [S2-S5](#)).

~~Direct comparison of the spatial distributions of species richness and expected number of links showed some areas with mismatches, both regarding the median estimates and regarding the within-ecoregion variability (Fig. ??). Median values for the ecoregions showed a similar bivariate distribution, with ecoregions in the south mostly displaying high species richness and a high number of links (Fig. ??A). The northernmost ecoregions (Canadian High Arctic Tundra and Davis Highlands Tundra) displayed higher richness (based on the quantile rank) compared to the number of links. Inversely, ecoregions further south (Canadian Low Arctic Tundra, Northern Canadian Shield Taiga, Southern Hudson Bay Taiga) ranked higher for the number of links than for species richness. On the other hand, within-ecoregion variability showed different bivariate relationships and a less constant latitudinal gradient (Fig. ??B). This indicates that richness and links do not co-vary completely (i.e. their variability is not highly correlated) although they may show similar distributions for median values [S3-S6](#).~~

Our results also indicate a mismatch between the uniqueness of communities and networks (Fig. 3). Uniqueness was higher mostly in the north and along the south border for communities, but ~~only~~ mostly in the north for networks (Fig. 3A-B). Consequently, ecoregions with both unique community composition and unique network composition were mostly in the north (Fig. 3C). Meanwhile, some areas were unique for one element but not the other. For instance, ~~the New England-Acadian forests ecoregion (south-east, near 70°W and 48°N) had a highly~~ ecoregions along the south border had a unique species composition but a more common network composition (Fig. 3C). ~~Opposite areas with~~ Two ecoregions showed the opposite (unique network compositions only ~~were observed at higher between latitudes 52°N and~~) at higher latitudes (Davis Highlands tundra, near 70°N (Eastern Canadian Shield Taiga, Northern Canadian Shield Taiga, Canadian Low Arctic Tundra). Also, and Southern Hudson Bay taiga, near 54°N).

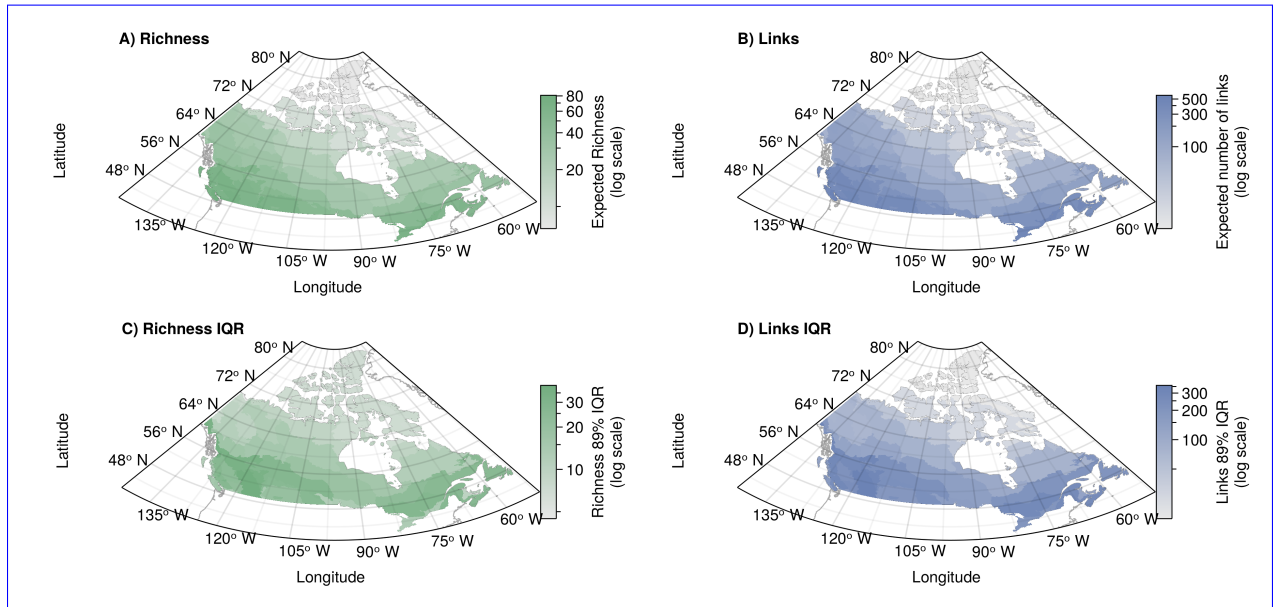


Figure 2: (A-B) Example of a community measure (A, expected species richness) and a network one (B, expected number of links). Both measures are assembled from the predicted probabilistic communities and networks, respectively. Values are first measured separately for all sites; then, the median value within each ecoregion was taken to represent the ecoregion-level value. (C-B) Representation of the 89% interquantile range of values within the ecoregion for expected richness (C) and expected number of links (D). All color bars follow a log scale with tick marks representing even intervals. Real values (non-log transformed) are shown beside major tick marks while minor ticks represent half increments.

Moreover, network uniqueness values for ecoregions spanned a narrower range between the 44 ecoregions than species LCBD values (Fig. 3D, left). Within-ecoregion variation was also lower for network values with generally lower 89% interquantile ranges among the site-level LCBD values (Fig. 3D, right). Moreover, mismatched sites (unique for only one element) formed two distinct groups when evaluating the relationship between species richness and the number of links (see Supplementary Material, Fig.S5). The areas only unique for their species composition had both a high richness and number of links

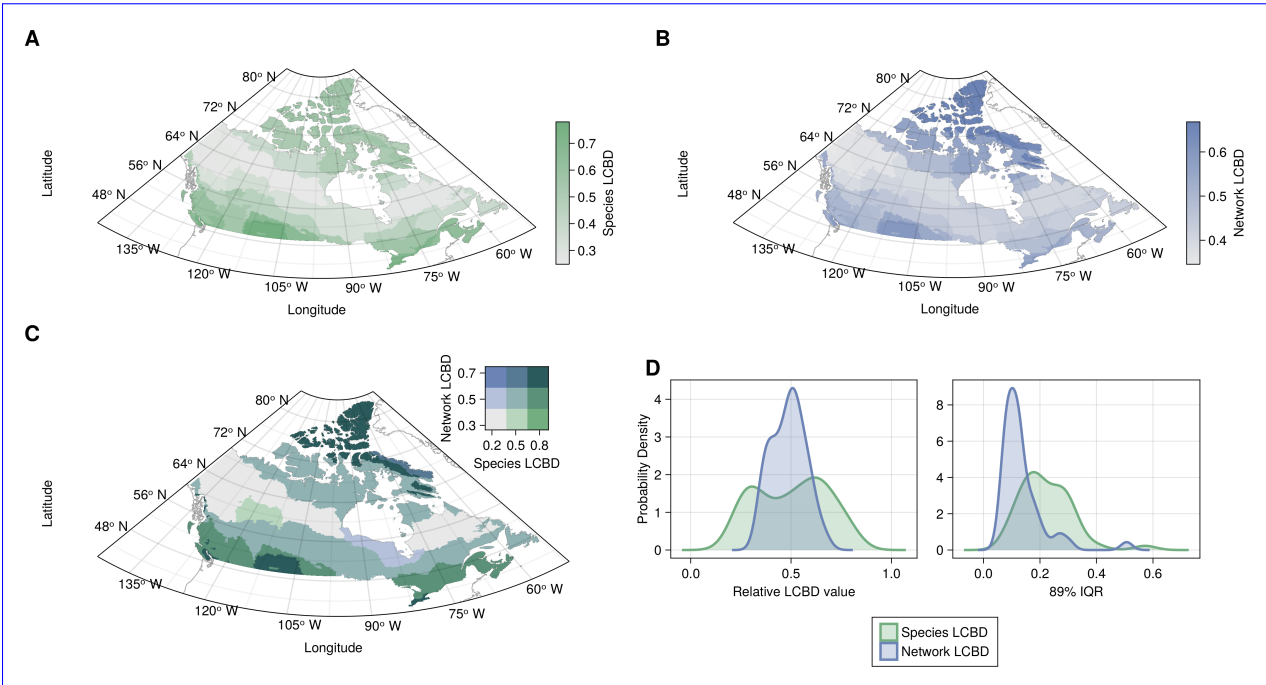


Figure 3: (A-B) Representation of the ecoregion uniqueness values based on species composition (A) and network composition (B). LCBD values were first computed across all sites and scaled relative to the maximum value observed. The ecoregion LCBD value is the median value for the sites in the ecoregion. (C) Bivariate representation of species and network composition LCBD. Values are grouped into three quantiles separately for each variable. The colour combinations represent the nine possible combinations of quantiles. The species uniqueness (horizontal axis) goes left to right from low uniqueness (light grey, bottom left) to high uniqueness (green, bottom right). The network composition uniqueness goes bottom-up from low uniqueness (light grey, bottom left) to high uniqueness (blue, top left). (D) Probability densities for the ecoregion LCBD values for species and network LCBD (left), highlighting the variability of LCBD values between ecoregions, and the 89% interquantile range of the values within each ecoregion (right), highlighting the variability within the ecoregions.

Comparing the distribution of dominant network motifs revealed additional areas of variation in network structure (Fig. 4). NDTI displayed a latitudinal gradient between the trophic motifs.

Northern ecoregions showed positive NDTI values and high dominance of S1 (tri-trophic chains) expected counts compared to S2 (omnivory) but ecoregions along the south border showed a reduced dominance (Fig. 4A). Ecoregions near the Ontario Peninsula and Saint-Lawrence Valley showed values close to zero, indicating a balance between two motifs, while Central New Brunswick had slightly negative values, indicating a low dominance of S2. In comparison, NDCI values showed an evenly high dominance of S5 (apparent competition) over S4 (exploitative competition) across all ecoregions (Fig. 4B). Meanwhile, within-ecoregion variance displayed a different spatial distribution from the median values. NDTI interquantile ranges spanned a wide range of values and were higher both in the north and in the south (although not in the ecoregions with higher NDTI median values) (Fig. 4C). On the other hand, ~~the sites only unique for their networks had both lower richness and a lower number of links, although they were not the sites with the lowest values for both~~ NDCI interquantile ranges showed lower within-ecoregion variance in most ecoregions except in the northernmost one (Canadian High Arctic tundra), which has a notably higher value (Fig. 4D). Although this higher variance does not reflect in the NDCI median values, it does appear when looking at the site-level values, where this ecoregion is the only one with patches with high positive NDCI values (indicating a dominance of S4) surrounded by highly negative values (indicating a dominance of S5) as in other ecoregions (Fig. S6B).

Discussion

Our approach presents a way to downscale a metaweb, produce localized predictions using probabilistic networks as inputs and outputs, and incorporate uncertainty, as called for by Strydom *et al.* (2023). It gives us an idea of what local metawebs or networks could look like in space, given species distributions and their variability, as well as the uncertainty around species interactions. We also provide the first spatial representation of the metaweb of Canadian mammals (Strydom *et al.* 2022) and a probabilistic equivalent to how the European tetrapod metaweb (Maiorano *et al.* 2020) was used to predict localized

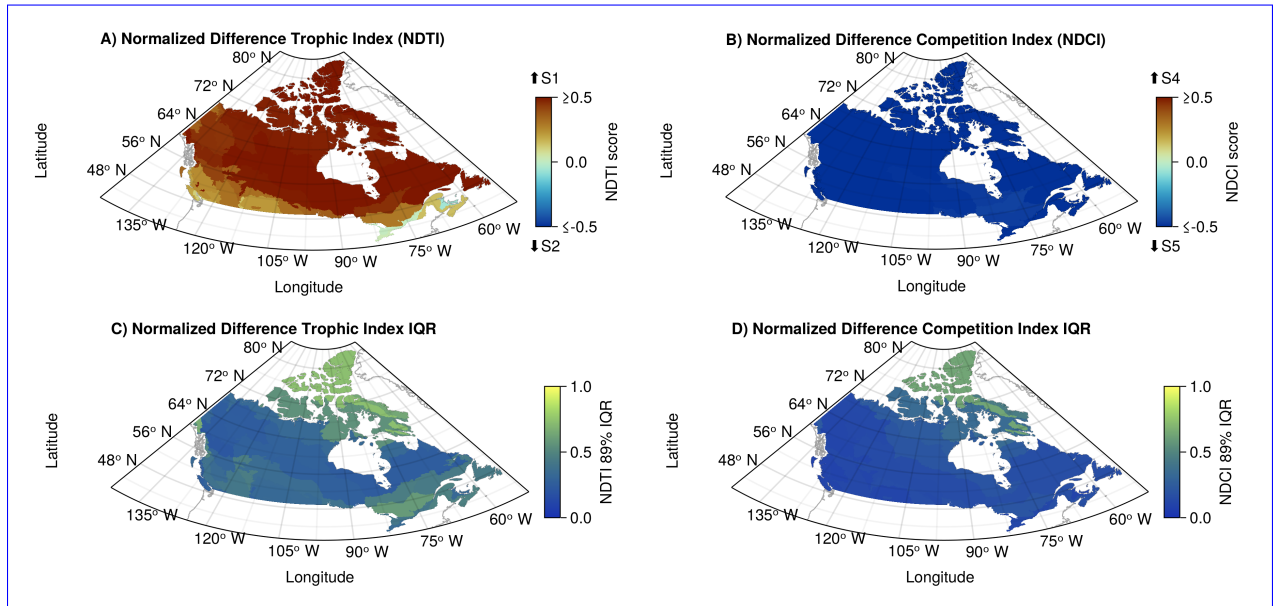


Figure 4: Comparison of the dominant ecological motifs across ecoregions. A) Normalized Difference Index (NDTI) comparing the trophic motifs S1 (tri-trophic food chains) and S2 (omnivory). Positive values indicate a dominance of S1 while negative values indicate a dominance of S2. Values equal or superior to $|0.5|$ are shown with the same color as they indicate a high dominance of one motif. B) Normalized Difference Index (NDCI) comparing the competition motifs S4 (exploitative competition) and S5 (apparent competition). Positive values indicate a dominance of S4 while negative values indicate a dominance of S5. (C-D) Representation of the 89% interquartile range of values within the ecoregion for the trophic motifs index (NDTI, C) and competition motifs index (NDCI, D).

networks in Europe (Braga *et al.* 2019; O'Connor *et al.* 2020; Galiana *et al.* 2021; Gaüzère *et al.* 2022; Botella *et al.* 2023). Therefore, our approach could open similar possibilities of investigations on the variation of structure in space (Braga *et al.* 2019) and on the effect of land-use intensification (Botella *et al.* 2023) on North American food webs, particularly Canadian mammal food webs. Other interesting research applications include assessing climate change impacts on network structure (e.g., Kortsch *et al.* 2015) or investigating linkages between network structure and stability (Windsor *et al.* 2023).

As our approach is probabilistic, it does not assume species interact whenever they co-occur and incorporates variability based on environmental conditions (via projected species distributions), which could lead to different results by introducing a different association between species richness and network properties. Galiana *et al.* (2021) found that species richness had a large explanatory power over network properties, but mentioned this could potentially be due to interactions between species being constant across space.

Here, we found ~~mismatches in the distribution of~~ that potential species richness and ~~interactions that were especially apparent in their~~ number of links displayed similar distributions following a latitudinal gradient, but that the within-ecoregion ~~variability~~ variance was lower along the southern border than the measures themselves (Fig. ??), ~~highlighting that interactions might vary differently than species distributions even over continental-scale gradients.~~ Network 2). Why the relationship between the median ecoregion values and the ecoregion variance is not constant across space could be verified through more tests in future studies (for instance, testing the effect of higher urban density in the south). Examples of metaweb structure in space are rare and not ideal for comparison with our results. For instance, we found that network density (links on Fig. ??A) ~~were also~~ 2B) were lower in the north, ~~contrarily which is contrary~~ to what was observed ~~for all European terrestrial tetrapods in Europe for the terrestrial tetrapod metaweb~~ (Braga *et al.* 2019; Galiana *et al.* 2021) and for willow-galler-parasitoid networks (Gravel *et al.* 2019), where connectance was higher in northern regions. However, those are systems with different number of species and environmental conditions (e.g. Europe and Canada could

differ due to varying climatic conditions at the same latitudes). Further research should investigate why these results might differ between ~~the two continents and~~ continents and ecological systems and whether it is due to the methodology, data, or biogeographical processes.

Our LCBD and uniqueness results highlighted that areas with unique network composition differ from sites with unique species composition. In other words, the joint distribution of community and network uniqueness highlights different diversity hotspots. Poisot *et al.* (2017) showed a similar result with host-parasite communities of rodents and ectoparasitic fleas. Our results further show ~~how that~~ these differences could be distributed across ecoregions and ~~in over~~ a broad spatial extent ~~. Areas unique for only one element (species or network composition) differed in their combination of species richness and number of links (Supplementary Material, Fig. S5), with species-unique sites displaying high values of both measures, and network-unique sites displaying low values. Moreover, for mammal~~ food webs. LCBD scores essentially highlight variability hotspots and are a measure of the variance of community or network structure. Here, they also serve as an inter-ecoregion variation measure, which can be compared to the within-ecoregion variation highlighted by the interquantile ranges. The narrower range of values for network LCBD values and the lower IQR values indicate that both the inter-ecoregion and within-ecoregion variation are lower for networks than for species (Fig. 3). ~~Additionally, higher values for network LCBD also indicate that most ecoregions can hold ecologically unique sites~~

Our analysis of the distribution of dominant network motifs revealed additional areas of variation in network structure. Trophic motifs (S1 and S2, measured through NDTI values) showed a latitudinal gradient different from the richness and links ones, with high dominance of tri-trophic chains (S1) in the north and higher omnivory counts (S2) only in a few ecoregions in the south. This results did not seem related to ecoregion variance, which once again showed a very different distribution from the median values. Meanwhile, competition motifs (S4 and S5, measured through NDCI values) showed an even dominance of apparent competition (S5) but high variance in a single ecoregion. Overall, our results

show that dominant motifs within a mammal food web vary between ecoregions and vary differently across space.

When to use the workflow we presented here will depend on the availability of interaction data or existing metawebs, and on the intent to incorporate interaction variability, as well as ecoregion-level variability. In systems where *in situ* interaction and complete network data are available, the approach put forward by Gravel *et al.* (2019) achieves a similar purpose as we attempted here, but is more rigorous and allows modelling the effect of the environment on the interactions themselves. Without such data, establishing or predicting the metaweb (e.g. using transfer learning) should be the first step toward producing localized predictions (Strydom *et al.* 2023). Our framework then downscales the metaweb towards the localized predictions, here using the probabilistic Canadian mammal one, but it can also use other metawebs generated through various means. Well-documented binary ~~metawebs~~-ones such as the European tetrapod metaweb could be partly combined with our approach if used with probabilistic SDMs and summarized by ecoregions (as they would only lack an initial probabilistic metaweb, but would still obtain a more probabilistic output). Our approach will essentially differ from previous attempts in how it perceives uncertainty and variability. For instance, rare interactions should not be over-represented (Poisot *et al.* 2016) and should have lesser effects over computed network measures. Furthermore, summarizing results by ecoregion allows for showing variation within and between ecologically meaningful biogeographic boundaries (Martins *et al.* 2022), which, as our results showed, is not constant across space and can help identify contrasting diversity hotspots.

Adding validation to our framework will be highly important for the predictions to be actionable. We see it as the next step since data availability currently remains an issue. Developing a way to generate actionable information when information is initially scarce, as we present here, is highly important in itself. Our manuscript highlights the application of a predictive pipeline in a case where interactions are almost fully predicted, but it can equally be applied when there are additional data about the interaction

network. Moreover, the predictions we make are already actionable, as any future sampling of food
web structure can be used to validate them, and fed into the model to iterate these results again. As
Strydom *et al.* (2023) point out, validation of metaweb predictions, empirical sampling, and method
design should all proceed jointly, and making conceptual progress in one of these areas helps all the
others.

The recent shift in focus towards building metawebs opens many opportunities for projections of networks in space through probabilistic downscaling, as we suggested here. Metawebs have been documented in many systems, allowing us to build new ones from predictions. How the European tetrapod metaweb (Maiorano *et al.* 2020) was used to predict the Canadian mammal metaweb (Strydom *et al.* 2022) is one such case, but recent examples also extend to other systems. Metawebs have been compiled for many marine food webs (e.g., Barents Sea, Kortsch *et al.* 2019; North Scotia Sea, López-López *et al.* 2022; Gulf of Riga, Kortsch *et al.* 2021) and used to predict the probability of novel interactions (Arctic food web of the Barents sea, Pecuchet *et al.* 2020). Olivier *et al.* (2019) built a temporally resolved metaweb of demersal fish and benthic epifauna but also suggested combining their approach with techniques estimating the probability of occurrence of trophic relationships to describe spatial and temporal variability more accurately. Lurgi *et al.* (2020) built a metaweb and probabilistic (occurrence-based) networks for rocky intertidal communities (and doing so they also showed that environmental factors do not affect the structure of binary and probabilistic networks in different ways). Albouy *et al.* (2019) predicted the global marine fish food web using a probabilistic model, showing the potential to describe networks across broad spatial scales. Similarly, predictive approaches are also increasingly used with other interaction types to highlight interactions hotspots on global scales (e.g. mapping geographical hotspots of predicted host-virus interactions between bats and betacoronaviruses, Becker *et al.* 2022; predicting the distribution of hidden interactions in the mammalian virome, Poisot *et al.* 2023). Our workflow offers the potential to bring these global predictions down to the local scale where they can be made more actionable, and

486 vastly increases the diversity of ecological networks that can be projected in space.

487 **Acknowledgements**

488 We acknowledge that this study was conducted on land within the traditional unceded territory of the
489 Saint Lawrence Iroquoian, Anishinabewaki, Mohawk, Huron-Wendat, and Omàmiwininiwak nations.
490 GD is funded by the NSERC Postgraduate Scholarship – Doctoral (grant ES D – 558643), the FRQNT
491 doctoral scholarship (grant no. 301750), and the NSERC CREATE BIOS² program. TP is funded by
492 the Wellcome Trust (223764/Z/21/Z), NSERC through the Discovery Grant and Discovery Accelerator
493 Supplements programs, and the Courtois Foundation. This research was enabled in part by support
494 provided by Calcul Québec (calculquebec.ca) and the Digital Research Alliance of Canada (alliancecan
495 .ca) through the Narval general purpose cluster.

References

- Albouy, C., Archambault, P., Appeltans, W., Araújo, M.B., Beauchesne, D., Cazelles, K., *et al.* (2019). The marine fish food web is globally connected. *Nature Ecology & Evolution*, 3, 1153–1161.
- [Baiser, B., Elheshha, R. & Kahveci, T. \(2016\). Motifs in the assembly of food web networks. *Oikos*, 125, 480–491.](#)
- [Baiser, B., Gravel, D., Cirtwill, A.R., Dunne, J.A., Fahimipour, A.K., Gilarranz, L.J., *et al.* \(2019\). Ecogeographical rules and the macroecology of food webs. *Global Ecology and Biogeography*, geb.12925.](#)
- [Baker, N.J., Kaartinen, R., Roslin, T. & Stouffer, D.B. \(2015\). Species' roles in food webs show fidelity across a highly variable oak forest. *Ecography*, 38, 130–139.](#)
- [Barbet-Massin, M., Jiguet, F., Albert, C.H. & Thuiller, W. \(2012\). Selecting pseudo-absences for species distribution models: How, where and how many? *Methods in Ecology and Evolution*, 3, 327–338.](#)
- [Becker, D.J., Albery, G.F., Sjodin, A.R., Poisot, T., Bergner, L.M., Chen, B., *et al.* \(2022\). Optimising predictive models to prioritise viral discovery in zoonotic reservoirs. *The Lancet Microbe*, 3, e625–e637.](#)
- [Bezanson, J., Edelman, A., Karpinski, S. & Shah, V.B. \(2017\). Julia: A fresh approach to numerical computing. *SIAM Review*, 59, 65–98.](#)
- [Botella, C., Gaüzère, P., O'Connor, L., Ohlmann, M., Renaud, J., Dou, Y., *et al.* \(2023\). Land-use intensity influences European tetrapod food-webs \(Preprint\). Authorea.](#)
- [Braga, J., Pollock, L.J., Barros, C., Galiana, N., Montoya, J.M., Gravel, D., *et al.* \(2019\). Spatial analyses of multi-trophic terrestrial vertebrate assemblages in Europe. *Global Ecology and Biogeography*, 28, 1636–1648.](#)
- [Cirtwill, A.R. & Stouffer, D.B. \(2015\). Concomitant predation on parasites is highly variable but constrains the ways in which parasites contribute to food web structure. *Journal of Animal Ecology*, 84, 734–744.](#)

da Silva, P.G. & Hernández, M.I.M. (2014). Local and regional effects on community structure of dung
pre

beetles in a mainland-island scenario. *PLOS ONE*, 9, e111883.

Danisch, S. & Krumbiegel, J. (2021). Makie.jl: Flexible high-performance data visualization for Julia.

Journal of Open Source Software, 6, 3349.

Dansereau, G., Legendre, P. & Poisot, T. (2022). Evaluating ecological uniqueness over broad spatial

extents using species distribution modelling. *Oikos*, 2022, e09063.

Dansereau, G. & Poisot, T. (2021). SimpleSDMLayers.jl and GBIF.jl: A framework for species distribution

modeling in Julia. *Journal of Open Source Software*, 6, 2872.

Dansereau, G. & Poisot, T. (2023). PoisotLab/SpatialProbabilisticMetaweb: V1.0.

Desjardins-Proulx, P., Laigle, I., Poisot, T. & Gravel, D. (2017). Ecological interactions and the Netflix
pre

problem. *PeerJ*, 5, e3644.

Dinerstein, E., Olson, D., Joshi, A., Vynne, C., Burgess, N.D., Wikramanayake, E., *et al.* (2017). An

Ecoregion-Based Approach to Protecting Half the Terrestrial Realm. *BioScience*, 67, 534–545.

Dunne, J. (2006). The network structure of food webs. In: *Ecological Networks: Linking Structure to*

Dynamics in Food Webs. pp. 27–86.

Frelat, R., Kortsch, S., Kröncke, I., Neumann, H., Nordström, M.C., Olivier, P.E.N., *et al.* (2022). Food

web structure and community composition: A comparison across space and time in the North Sea.

Ecography, 2022.

Galiana, N., Barros, C., Braga, J., Ficetola, G.F., Maiorano, L., Thuiller, W., *et al.* (2021). The spatial

scaling of food web structure across European biogeographical regions. *Ecography*, 44, 653–664.

Galiana, N., Lurgi, M., Bastazini, V.A.G., Bosch, J., Cagnolo, L., Cazelles, K., *et al.* (2022). Ecological

network complexity scales with area. *Nature Ecology & Evolution*, 1–8.

Gaüzère, P., O'Connor, L., Botella, C., Poggiato, G., Münkemüller, T., Pollock, L.J., *et al.* (2022). The di-

542 iversity of biotic interactions complements functional and phylogenetic facets of biodiversity. *Current*
543 *Biology*.

544 GBIF Secretariat. (2021). GBIF Backbone Taxonomy.

545 GBIF.org. (2022). GBIF occurrence download.

546 GDAL/OGR contributors. (2021). *GDAL/OGR geospatial data abstraction software library*. Manual.

547 Open Source Geospatial Foundation.

548 Gravel, D., Baiser, B., Dunne, J.A., Kopelke, J.-P., Martinez, N.D., Nyman, T., *et al.* (2019). Bringing

549 Elton and Grinnell together: A quantitative framework to represent the biogeography of ecological
550 interaction networks. *Ecography*, 42, 401–415.

551 Guisan, A. & Thuiller, W. (2005). Predicting species distribution: Offering more than simple habitat
552 models. *Ecology Letters*, 8, 993–1009.

553 Heino, J. & Grönroos, M. (2017). Exploring species and site contributions to beta diversity in stream
554 insect assemblages. *Oecologia*, 183, 151–160.

555 Hortal, J., de Bello, F., Diniz-Filho, J.A.F., Lewinsohn, T.M., Lobo, J.M. & Ladle, R.J. (2015). Seven
556 Shortfalls that Beset Large-Scale Knowledge of Biodiversity. *Annual Review of Ecology, Evolution,*
557 *and Systematics*, 46, 523–549.

558 Jordano, P. (2016). Sampling networks of ecological interactions. *Functional Ecology*, 30, 1883–1893.

559 Karger, D.N., Conrad, O., Böhner, J., Kawohl, T., Kreft, H., Soria-Auza, R.W., *et al.* (2017). Climatologies
560 at high resolution for the earth’s land surface areas. *Scientific Data*, 4, 170122.

561 Karger, D.N., Conrad, O., Böhner, J., Kawohl, T., Kreft, H., Soria-Auza, R.W., *et al.* (2018). Data from:
562 Climatologies at high resolution for the earth’s land surface areas.

563 Karger, D.N., Conrad, O., Böhner, J., Kawohl, T., Kreft, H., Soria-Auza, R.W., *et al.* (2021). Climatologies
564 at high resolution for the earth’s land surface areas.

565 Kortsch, S., Frelat, R., Pecuchet, L., Olivier, P., Putnis, I., Bonsdorff, E., *et al.* (2021). Disentangling

temporal food web dynamics facilitates understanding of ecosystem functioning. *Journal of Animal Ecology*, 90, 1205–1216.

Kortsch, S., Primicerio, R., Aschan, M., Lind, S., Dolgov, A.V. & Planque, B. (2019). Food-web structure varies along environmental gradients in a high-latitude marine ecosystem. *Ecography*, 42, 295–308.

Kortsch, S., Primicerio, R., Fossheim, M., Dolgov, A.V. & Aschan, M. (2015). Climate change alters the structure of arctic marine food webs due to poleward shifts of boreal generalists. *Proceedings of the Royal Society B: Biological Sciences*, 282, 20151546.

Legendre, P. & De Cáceres, M. (2013). Beta diversity as the variance of community data: Dissimilarity coefficients and partitioning. *Ecology Letters*, 16, 951–963.

López-López, L., Genner, M.J., Tarling, G.A., Saunders, R.A. & O’Gorman, E.J. (2022). Ecological Networks in the Scotia Sea: Structural Changes Across Latitude and Depth. *Ecosystems*, 25, 457–470.

Lucas, P., Thuiller, W., Talluto, M., Polaina, E., Albrecht, J., Selva, N., *et al.* (2023). Including biotic interactions in species distribution models improves the understanding of species niche: A case of study with the brown bear in Europe.

Lurgi, M., Galiana, N., Broitman, B.R., Kéfi, S., Wieters, E.A. & Navarrete, S.A. (2020). Geographical variation of multiplex ecological networks in marine intertidal communities. *Ecology*, 101, e03165.

Maiorano, L., Montemaggiori, A., Ficetola, G.F., O’Connor, L. & Thuiller, W. (2020). TETRA-EU 1.0: A species-level trophic metaweb of European tetrapods. *Global Ecology and Biogeography*, 29, 1452–1457.

Martins, L.P., Stouffer, D.B., Blendinger, P.G., Böhning-Gaese, K., Buitrón-Jurado, G., Correia, M., *et al.* (2022). Global and regional ecological boundaries explain abrupt spatial discontinuities in avian frugivory interactions. *Nature Communications*, 13, 6943.

McElreath, R. (2020). *Statistical rethinking: A bayesian course with examples in R and Stan*. Second. Chapman and Hall/CRC, New York.

McLeod, A., Leroux, S.J., Gravel, D., Chu, C., Cirtwill, A.R., Fortin, M.-J., *et al.* (2021). Sampling and asymptotic network properties of spatial multi-trophic networks. *Oikos*, 130, 2250–2259.

Mestre, F., Gravel, D., García-Callejas, D., Pinto-Cruz, C., Matias, M.G. & Araújo, M.B. (2022). Disentangling food-web environment relationships: A review with guidelines. *Basic and Applied Ecology*, 61, 102–115.

Milo, R., Shen-Orr, S., Itzkovitz, S., Kashtan, N., Chklovskii, D. & Alon, U. (2002). Network Motifs: Simple Building Blocks of Complex Networks. *Science*, 298, 824–827.

Moens, M., Biesmeijer, J., Huang, E., Vereecken, N. & Marshall, L. (2022). The importance of biotic interactions in distribution models depends on the type of ecological relations, spatial scale and range.

Mora, B.B., Gravel, D., Gilarranz, L.J., Poisot, T. & Stouffer, D.B. (2018). Identifying a common backbone of interactions underlying food webs from different ecosystems. *Nature Communications*, 9, 2603.

Morales-Castilla, I., Matias, M.G., Gravel, D. & Araújo, M.B. (2015). Inferring biotic interactions from proxies. *Trends in Ecology & Evolution*, 30, 347–356.

O'Connor, L.M.J., Pollock, L.J., Braga, J., Ficetola, G.F., Maiorano, L., Martinez-Almoyna, C., *et al.* (2020). Unveiling the food webs of tetrapods across Europe through the prism of the Eltonian niche. *Journal of Biogeography*, 47, 181–192.

Olivier, P., Frelat, R., Bonsdorff, E., Kortsch, S., Kröncke, I., Möllmann, C., *et al.* (2019). Exploring the temporal variability of a food web using long-term biomonitoring data. *Ecography*, 42, 2107–2121.

Pecuchet, L., Blanchet, M.-A., Frainer, A., Husson, B., Jørgensen, L.L., Kortsch, S., *et al.* (2020). Novel feeding interactions amplify the impact of species redistribution on an Arctic food web. *Global Change Biology*, 26, 4894–4906.

Poggiato, G., Andréoletti, J., Shirley, L. & Thuiller, W. (2022). *Integrating food webs in species distribution*

models improves ecological niche estimation and predictions (Preprint). Authorea.

Poisot, T., Bélisle, Z., Hoebeke, L., Stock, M. & Szefer, P. (2019). EcologicalNetworks.jl: Analysing ecological networks of species interactions. *Ecography*, 42, 1850–1861.

Poisot, T., Bergeron, G., Cazelles, K., Dallas, T., Gravel, D., MacDonald, A., *et al.* (2021). Global knowledge gaps in species interaction networks data. *Journal of Biogeography*, 48, 1552–1563.

Poisot, T., Canard, E., Mouillot, D., Mouquet, N. & Gravel, D. (2012). The dissimilarity of species interaction networks. *Ecology Letters*, 15, 1353–1361.

Poisot, T., Cirtwill, A.R., Cazelles, K., Gravel, D., Fortin, M.-J. & Stouffer, D.B. (2016). The structure of probabilistic networks. *Methods in Ecology and Evolution*, 7, 303–312.

Poisot, T., Guéveneux-Julien, C., Fortin, M.-J., Gravel, D. & Legendre, P. (2017). Hosts, parasites and their interactions respond to different climatic variables. *Global Ecology and Biogeography*, 26, 942–951.

Poisot, T., Ouellet, M.-A., Mollentze, N., Farrell, M.J., Becker, D.J., Brierley, L., *et al.* (2023). Network embedding unveils the hidden interactions in the mammalian virome. *Patterns*, 4, 100738.

Poisot, T., Stouffer, D.B. & Gravel, D. (2015). Beyond species: Why ecological interaction networks vary through space and time. *Oikos*, 124, 243–251.

Saravia, L.A., Marina, T.I., Kristensen, N.P., De Troch, M. & Momo, F.R. (2022). Ecological network assembly: How the regional metaweb influences local food webs. *Journal of Animal Ecology*, 91, 630–642.

Simmons, B.I., Cirtwill, A.R., Baker, N.J., Wauchope, H.S., Dicks, L.V., Stouffer, D.B., *et al.* (2019). Motifs in bipartite ecological networks: Uncovering indirect interactions. *Oikos*, 128, 154–170.

Statistics Canada. (2022). *Boundary files, reference guide second edition, Census year 2021*. Second edition. pre

Statistics Canada = Statistique Canada, Ottawa.

Stouffer, D.B. & Bascompte, J. (2010). Understanding food-web persistence from local to global scales. *Ecology Letters*, 13, 154–161.

Stouffer, D.B., Camacho, J., Jiang, W. & Nunes Amaral, L.A. (2007). Evidence for the existence of a
robust pattern of prey selection in food webs. *Proceedings of the Royal Society B: Biological Sciences*,
274, 1931–1940.

Strydom, T., Bouskila, S., Banville, F., Barros, C., Caron, D., Farrell, M.J., *et al.* (2022a). Food
web reconstruction through phylogenetic transfer of low-rank network representation. *Methods in
Ecology and Evolution*, 13, 2838–2849.

Strydom, T., Bouskila, S., Banville, F., Barros, C., Caron, D., Farrell, M.J., *et al.* (2022b). Predicting
metawebs: Transfer of graph embeddings can help alleviate spatial data deficiencies (2023). Graph
embedding and transfer learning can help predict potential species interaction networks despite
data limitations. *Methods in Ecology and Evolution*, 14, 2917–2930.

Strydom, T., Catchen, M.D., Banville, F., Caron, D., Dansereau, G., Desjardins-Proulx, P., *et al.* (2021).
A roadmap towards predicting species interaction networks (across space and time). *Philosophical
Transactions of the Royal Society B: Biological Sciences*, 376, 20210063.

Tuanmu, M.-N. & Jetz, W. (2014). A global 1-km consensus land-cover product for biodiversity and
ecosystem modelling. *Global Ecology and Biogeography*, 23, 1031–1045.

Vasconcelos, T.S., Nascimento, B.T.M. do & Prado, V.H.M. (2018). Expected impacts of climate change
threaten the anuran diversity in the Brazilian hotspots. *Ecology and Evolution*, 8, 7894–7906.

Windsor, F.M., van den Hoogen, J., Crowther, T.W. & Evans, D.M. (2023). Using ecological networks to
answer questions in global biogeography and ecology. *Journal of Biogeography*, 50, 57–69.

Wisn, M.S., Pottier, J., Kissling, W.D., Pellissier, L., Lenoir, J., Damgaard, C.F., *et al.* (2013). The role
of biotic interactions in shaping distributions and realised assemblages of species: Implications for
species distribution modelling. *Biological Reviews*, 88, 15–30.

Youden, W.J. (1950). Index for rating diagnostic tests. *Cancer*, 3, 32–35.

660 Zarnetske, P.L., Baiser, B., Strecker, A., Record, S., Belmaker, J. & Tuanmu, M.-N. (2017). The Interplay
661 Between Landscape Structure and Biotic Interactions. *Current Landscape Ecology Reports*, 2, 12–29.